文章编号：1001-4888(2017)05-0634-11

Thickness effect on microstructural and mechanical properties of pulse-laser treated Ti/Ni multilayer thin films*

Zhou Yang, Melicent Stossel, Junlan Wang

(Department of Mechanical Engineering, University of Washington, Box 352600 Seattle, WA 98195, USA)

Abstract: Previous work showed that pulse-laser irradiation can strengthen metal multilayer thin films through intermetallic formation and the degree of strengthening is a function of laser pulse energy. In this work, the effect of individual layer thickness (λ) and total multilayer thickness (h) on the resulting microstructure and mechanical strength of laser-treated Ti/Ni multilayers was further investigated. Experiments were carried out on four λ/h combinations using individual layer thickness of 20nm and 50nm, and total multilayer thickness of 500nm and 1μm, respectively. Obvious intermetallic strengthening was observed in the 500nm thick multilayers, especially with the 20nm layer thickness, but not in the 1μm thick multilayers. Further, the multilayer surface morphology after laser treatment was observed to be dominated by competition between laser-induced optical interference and thermal melting, with the former leading to ripple or cross-hatched patterns and the latter leading to melted surfaces with pores and cracks.

Keywords: Ti/Ni multilayer; laser treatment; thickness effect; hardness; pulse-energy

CLC number: O34 **Document code**: A DOI: 10.7520/1001-4888-17-311

0 Introduction

Laser treatment has attracted renewed attention for various types of materials. For example, laser-induced periodic surface structures (LIPSS) on metals[1-3], semiconductors[4-6], and dielectrics[7,8] have been extensively studied and found potential applications in Micro/Nano-Electro-Mechanical Systems (MEMS/NEMS)[9,10]. Nanoscale laser processing and micromachining of polymers[11] and biomaterials[12,13] have been developed for electronic, optical and sensing applications. In addition, laser treatment has been applied to metal alloys[14,15] to improve the surface mechanical integrity such as hardness[16], fatigue strength[17], wear[18] and corrosion[19] resistances, via modification of phase composition and chemical state of the irradiated surfaces[20,21]. In contrast to bulk heat treatment, laser surface treatment is able to enhance surface properties while limiting the microstructure modification within a confined depth due to the short interaction time involved.

* 收稿日期：2017-07-21；修回日期：2017-09-01

通讯作者：Junlan Wang (1971—), PhD, is an Associate Professor in Mechanical Engineering. Her research interest is on the mechanics and physics of materials at small length scales, with a particular focus on the mechanics of thin films and coatings, biological and bio-inspired materials, and optics- and laser-based sensing and materials processing. Email: junlan@u.washington.edu

Nanoscale metallic multilayer thin films have been widely studied[22, 23] due to their superior functional (e.g. electric, magnetic and optical)[24, 25] as well as mechanical[26—29] properties compared to their monolithic counterparts. To our knowledge, our recent work was the first to demonstrate that when combined with laser surface treatment, mechanical properties of metal multilayers can be further enhanced due to a nanoscale intermixed coating formed on top of the surface[30]. This laser-treated multilayer has potential applications in various fields. For example: laser-treated multilayers with enhanced surface mechanical and tribological properties may be applied in electro-mechanical systems such as DC motors; laser-induced ultra-thin oxide protective coatings[31] can be used for biological/medical devices and act as diffusion barriers for corrosion resistance; laser-induced patterned surfaces[32] have applications in MEMS, semiconductor and photovoltaic industry, and superhydrophobic material systems[33]. Additionally, laser treatment on multilayer thin films can be a quick and convenient approach to obtain alloys or intermetallics[34, 35] which can significantly improve material magnetic[36] and mechanical properties[30].

Laser-induced microstructural evolution and functional property improvement of multilayer films can be significantly dependent on laser beam parameters, treatment environment, and characteristics of the materials. In our previous work, we studied the effect of laser pulse energy on microstructure evolution and surface strengthening of Ti/Ni multilayer thin films[30]. In this work, we will focus on the thickness effect on pulsed-laser treated Ti/Ni multilayer thin films including the effect from both individual layer thickness (λ), and total multilayer thickness (h) in order to have a better fundamental understanding of laser-induced surface strengthening of nanoscaled multilayer thin films.

1 Experimental details

Ti/Ni multilayer thin films were deposited on Si (100) substrates by a dual DC magnetron sputtering system (Orion-5-UHV from AJA International, Inc, MA). The Si substrates were cleaned by standard RCA cleaning and dipped in deionized water before deposition. Ti and Ni targets with 99.995% purity were used as sputtering source. The deposition was conducted in an Ar partial pressure of 5×10^{3} mbar and DC power of 100W for both Ti and Ni, with Ti deposited as the first layer and ending with Ni on the outermost top surface. The sputtering time of each layer was controlled to obtain the same layer thickness for both Ti and Ni. In this work, films with two individual layer thicknesses, 20nm and 50nm, and two total multilayer thicknesses, 1μm and 500nm, were deposited. Thus a total of 4 λ/h combinations were studied: 20nm/500nm, 20nm/1μm, 50nm/500nm, and 50nm/1μm.

The aforedeposited Ti/Ni multilayer thin films were subsequently irradiated using the same method as reported in our previous work[30]. Fig. 1 shows the schematic of the laser treatment setup and some representative surface morphologies of the treated Ti/Ni multilayer film from optical microscopy (OM), scanning electronic microscopy (SEM) and scanning probe microscopy (SPM). The Nd:YAG laser (Leopard SS-5, Continuum, Santa Clara, CA) was operated with 120 picosecond (ps) pulse duration and 1064nm wavelength. For the experiment in this work, the pulse energy was controlled from 25mJ to 125mJ, adjusted by the optical attenuator consisting of a half-wave plate and a linear polarizer. All film surfaces were treated with 50 successive pulses at a repetition rate of 5Hz. The linearly polarized laser beam was focused to a 3mm nominal diameter spot on the sample surface. In order to avoid excessive energy loss due to the high surface reflectivity, the sample was tilted to produce an incident angle of 67.5°, which resulted in an elliptical footprint on the sample surface with the short axis still being 3mm.

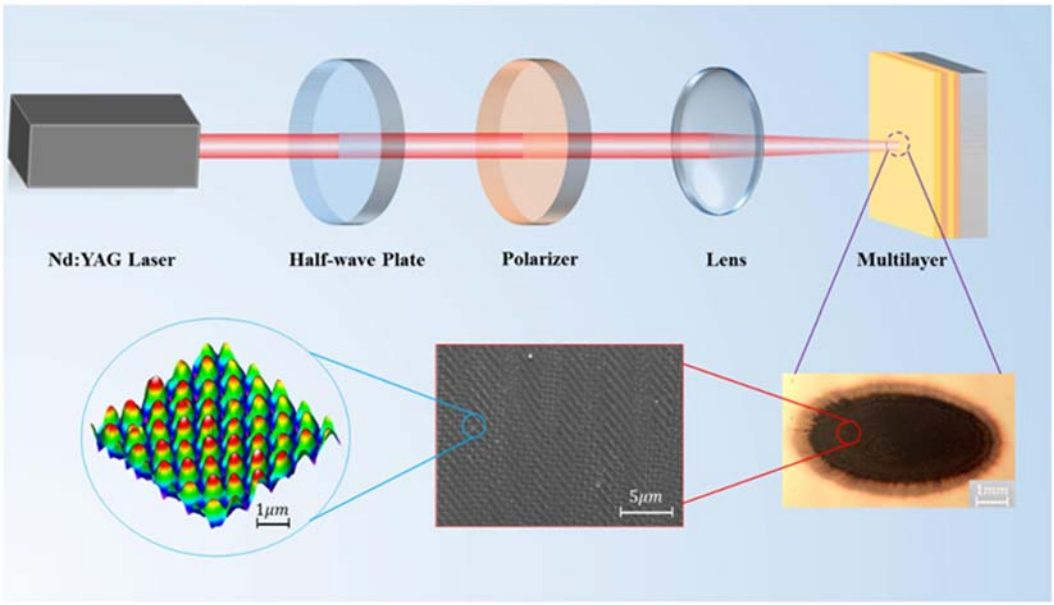

Fig. 1 Schematic of the laser treatment experiment and typical surface morphology after laser treatment obtained from SPM, SEM and OM

Detailed microstructure characterization was obtained using SEM (Sirion XL30, FEI) for surface and cross-sectional morphological evolution, and X-ray diffraction (XRD) (D8 Discover, Bruker) with Cu Kα radiation source and scan step of 0.06°/s for crystallinity and chemical state change.

Hardness was obtained by performing nanoindentation on the surface of both as-deposited and laser-treated Ti/Ni multilayer films. A Ubi1 nanomechanical test instrument (Hysitron, Inc., MN) with a Berkovich indenter tip was utilized to apply indents. Before and after indentation, an in-situ SPM imaging option was used to scan the surface and ascertain the indent quality. During indentation, a trapezoidal load function was applied with a 10s loading, 5s hold at maximum load, and 10s unloading. The resulting load-contact depth curve was then analyzed following a standard Oliver and Pharr method to obtain the hardness results[37]. For rough surfaces observed after high pulse-energy treatment, manual polishing was carried out before nanoindentation by using 0.3μm alumina slurry for about 30 seconds to remove a few nanometers of the rough asperities.

2 Results and discussions

2.1 Layer thickness effect on microstructural evolution

Previous study on the 20nm/500nm (λ/h) Ti/Ni multilayer thin films showed that laser pulse energy can have significant effect on the morphological evolution of laser treated multilayers[30]. With increasing pulse-energy, the cross-section morphology changes from a multilayered structure to a partially intermixed, then fully intermixed structure, and the surface morphology changes from a homogeneous grain structure to non-uniformly mixed surface structure with grains, ripples and lightly melted surface, then to a rough and heavily melted surface covered with voids and cracks. In the current work, the microstructural evolution of the 20nm/500nm and 50nm/500nm multilayers are compared in order to reveal the layer thickness effect.

Fig. 2 shows a side-by-side comparison of the cross-sectional morphology evolution of the 20nm/500nm and 50nm/500nm multilayers. The as-deposited samples both show clear layered structure with the darker layer being Ti and lighter layer Ni. After treatment with 50mJ laser energy, a thin (~50nm) and smooth intermixed layer was formed on the top of the multilayered film in the λ=20nm

case, while a thick (~100nm) and rough intermixed layer was observed in the λ=50nm case. After treatment with 75mJ, in the 20nm case, the intermixed layer becomes thicker (~100nm) and still uniformly overlays the multilayer surface while a fully intermixed structure was observed in the 50nm case. If the pulse-energy is increased to a higher level, similar fully intermixed structure will also be observed in the 20nm case, e. g. 100mJ and 125mJ[30].

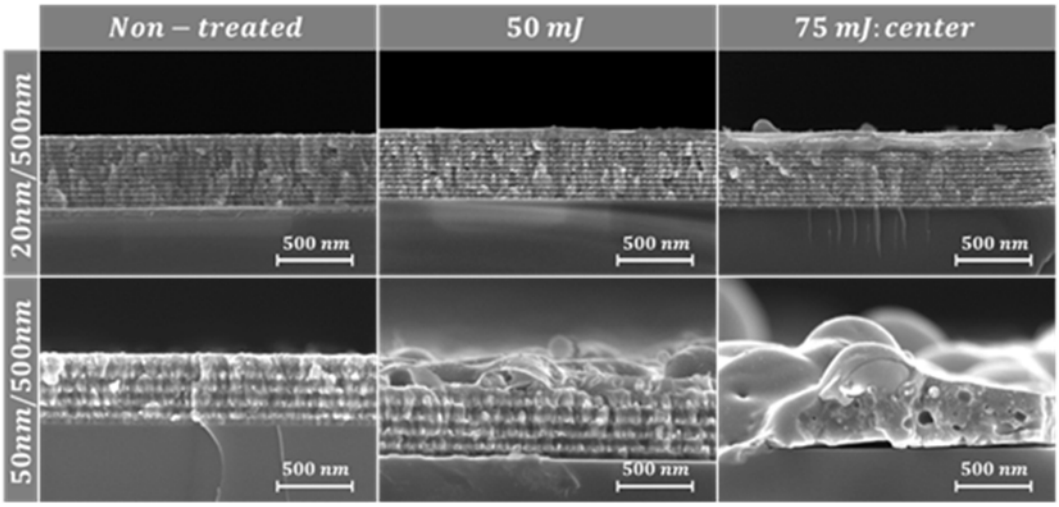

Fig. 2　Cross-sectional SEM images of non-treated and laser-treated 500nm thick Ti/Ni multilayer films with layer thickness of 20nm and 50nm, respectively

Fig. 3 shows the corresponding surface morphology evolution of the laser-treated 20nm/500nm and 50nm/500nm multilayers. The as-deposited samples both show a smooth surface with homogeneous grain distribution with grain size around 25nm. In the λ=20nm case, vertical ripples with a spacing around 250nm were observed on top of the grain surface when treated at 50mJ, and 45° ripples with a spacing around 700nm were observed when treated at 75mJ. These periodic ripple structures are indistinct and randomly distributed on the surfaces, which remain smooth or relatively smooth after laser treatment. After treatment with 100mJ pulse-energy, a rough and melted surface structure was observed. In the λ=50nm case, treatments with 50mJ and 75mJ pulse energy both led to rough and melted surfaces without any ripples. However, at a lower energy of 25mJ, a uniformly distributed vertical ripple structure with ripple spacing on the order of 100nm was observed. This new feature is likely a superposition between a LIPSS from the optical interference and a lightly melted surface as seen from the inset of the 25mJ treated image. It is interesting to note that three different types of ripples were observed with the same laser beam parameters.

Both cross-section and surface SEM images demonstrate significant layer thickness effect on the morphological evolution. Further investigation of layer-thickness dependent phase composition and chemical state after laser treatment was carried out using XRD. Fig. 4 shows XRD patterns before and after laser treatment for the 500nm thick films with λ=20nm and λ=50nm, respectively. Both as-deposited films show similar crystallinity: HCP Ti (100) structure and FCC Ni (111) structure. After treatment with 50mJ, a similar XRD pattern was observed in the 20nm case, indicating no obvious phase modification, while in the 50nm case the Ti peak almost disappeared and a tiny Ti-Ni intermetallic peak $NiTi_2$(400) was detected. The intermetallic peak becomes increasingly more intense at higher pulse-energy, and meanwhile more Ti-Ni intermetallic phases were detected. For the 20nm case, the intermetallic peak was first detected at 75mJ, which is higher than that in the 50nm case. The intermetallic peaks also become more intense at higher pulse-energy. For both the 20nm and

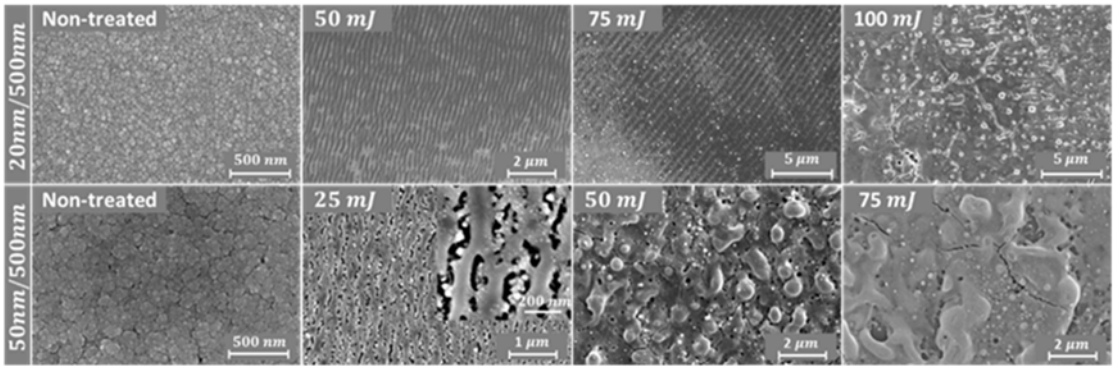

Fig. 3 Surface SEM images of non-treated and laser-treated 500nm thick Ti/Ni multilayer films with layer thickness of 20nm and 50nm, respectively

50nm cases, the Ti-Ni intermetallic evolution behavior is similar: intermetallic phase initially precipitates with a certain pulse-energy, with more precipitation and phases at higher pulse-energy. However, for the two different λ values, the Ti-Ni intermetallic phases are formed at different energies, indicating an important role played by the individual layer thickness. When the individual layer is thick, diffused Ni atoms could be surrounded by more Ti atoms, leading to the formation of intermetallic phase with higher Ti fraction, such as $NiTi_2$ in the 50nm case. When the individual layer is thin, full intermixing could occur more easily, promoting the formation of NiTi and Ni_4Ti_3, as in the 20nm case. Only a weak NiTi intermetallic peak was detected in a previously reported work with individual layer thickness of 16nm[34]. In addition, a TiO_2 phase was detected in the 50nm case. This oxide peak appeared after treatment with 75mJ and became more intense at higher pulse energy.

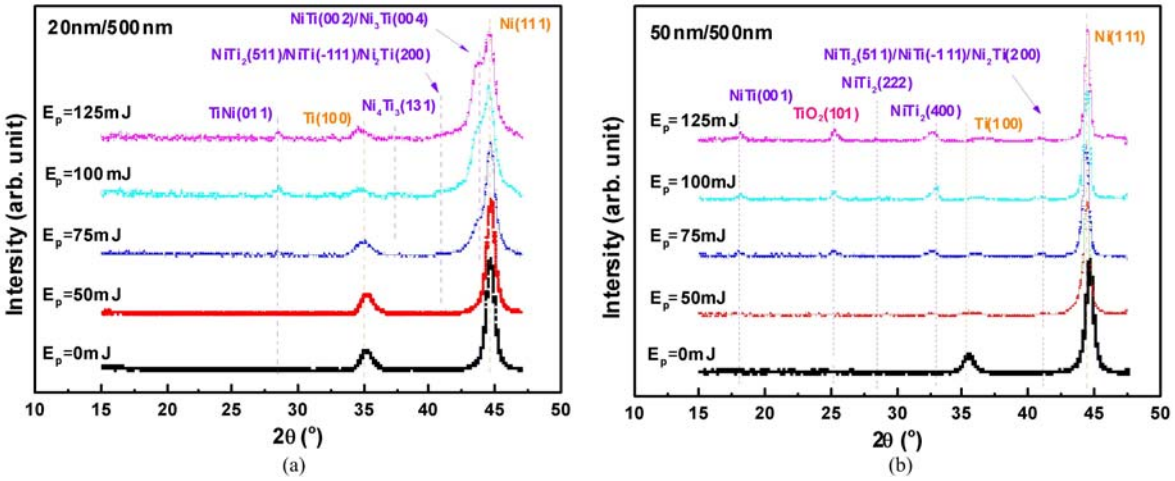

Fig. 4 XRD patterns for non-treated and laser-treated 500nm thick Ti/Ni multilayer films with layer thickness of (a) 20nm and (b) 50nm, respectively. In both figures, the symbol E_p refers to pulse-energy

2.2 Total film thickness effect on microstructural evolution

In addition to individual layer thickness, total film thickness (h) can also play an important role in the laser-treated multilayer microstructure evolution. In previous work, for example, laser-induced periodic surface structures were observed to have different spacing on irradiated surfaces for samples with different total film thickness[30]. In this work, different cross-section and surface morphologies have been observed in samples with different h. Fig. 5 shows the SEM morphology images after laser treatment with 50mJ and 75mJ on both the 500nm and 1μm thick films with λ=20nm and λ=50nm, respectively. From examination of the cross-sectional morphology, the 1μm film shows a thin and smooth intermixed structure uniformly distributed within the top layers of the multilayer. In

comparison, the 500nm film develops a thick and rough intermixed layer. Furthermore, even thicker intermixing can be observed in samples with $\lambda = 50$nm. The comparison of cross-sectional morphologies from all four cases indicates that more energy can be accumulated near surface with a larger λ/h ratio, which is also confirmed by the corresponding surface morphologies. With laser treatment after 75mJ, for example, the 50nm/500nm films showed a massively melted surface covered by bubbles, voids and cracks, the 20nm/500nm films displayed a mixed surface morphology with indistinct 45 ripples and locally melted surface, while the two 1μm films exibited a uniformly distributed cross-hatched patterned structure. In the current study, the cross-hatched patterns can be observed in the 1μm films even after treatment with pulse-energy as high as 125mJ, indicating that a wide range of pulse-energies could be used to obtain the periodic structure for thick films. In addition, in the 1μm thick films, the individual layer thickness effect on the cross-section and surface morphologies is not as significant as in the 500nm thick films. That is, for the 1μm films, the uniformly distributed intermixed layer and distinct cross-hatched surface pattern can be observed in both the 20nm and 50nm cases. Although not included here, the laser-treated 1μm thick Ti/Ni multilayers showed very similar XRD spectra to the non-treated samples, indicating that the accumulated energy in the intermixed layer is probably not sufficient to introduce any crystallinity or chemical state modification.

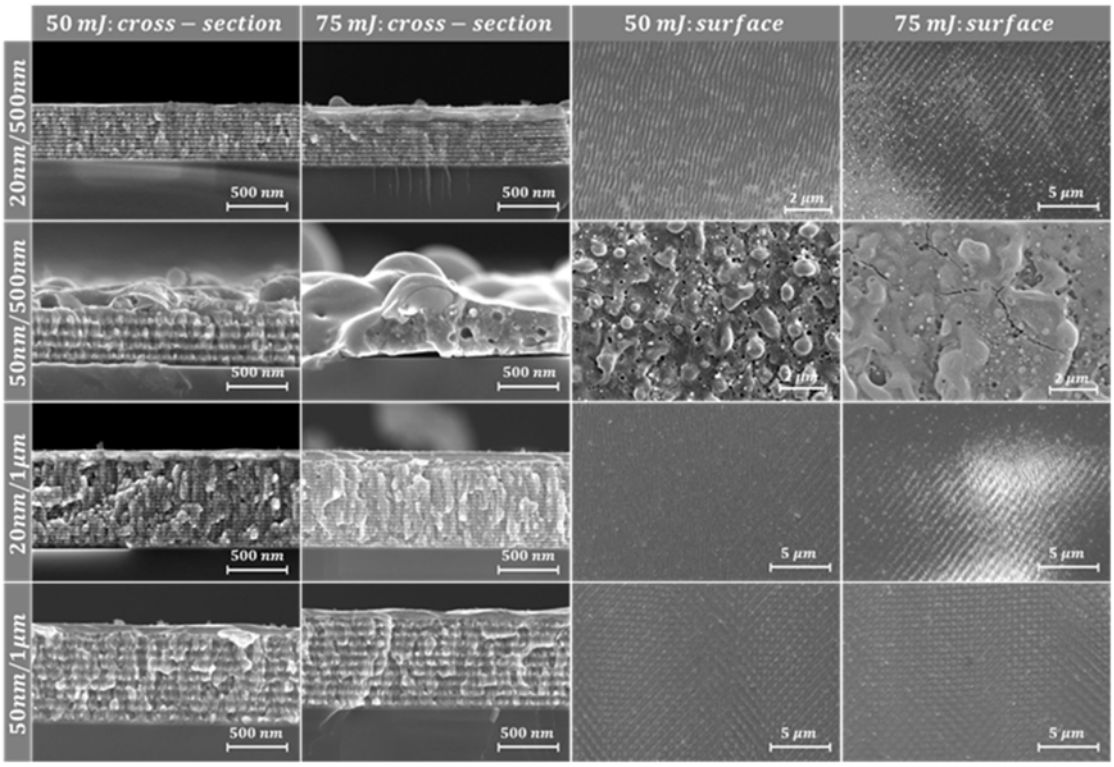

Fig. 5　Cross-section and surface SEM morphologies for 50mJ and 75mJ treated 500nm and 1μm thick Ti/Ni multilayer films with layer thicknesses of 20nm and 50nm, respectively

2.3　Hardness characterization

For films characterized in this work, the hardness was obtained following the same protocol as used in the previously work[30]. The indentation depth was all controlled below 30% of the total film thickness, and the hardness was averaged within the constant hardness vs contact depth range. Fig. 6 shows the hardness as a function of pulse-energy for all four sets of Ti/Ni multilayer thin films. The as-deposited Ti/Ni multilayers have hardness values around 5.8GPa for λ=20nm and 5.4GPa for λ=

50nm. In the 20nm/500nm case, no obvious hardness change is observed after laser treatment with 50mJ, while significant hardening is observed at higher pulse-energy in both unpolished and polished samples as shown in Fig. 6(a). For example, an estimated 25% hardness increase was measured after laser treatment with 100mJ. In the 50nm/500nm case, the surface was too rough to apply indentation after high energy treatment. Careful polishing was carried out to obtain locally smooth area for indentation. As shown in Fig. 6(b), polished samples displayed hardening after treatment with pulse-energy higher than 25mJ, although the increase is not as significant (around 5% after 50mJ treatment) as that in the 20nm/500nm case. For the 1μm thick films, since the treated surface was relatively smooth, polishing was not necessary. Different from the 500nm thick films, the 1μm thick films showed little hardness change after laser treatment from 25mJ to 100mJ, regardless of the layer thickness (20nm or 50nm). Note that the small hardness difference between polished and unpolished data in Fig. 6(a) could be due to polishing induced hardening[26]. However, this effect is not dominant and the trend of hardness evolution with increasing pulse energy is still clear.

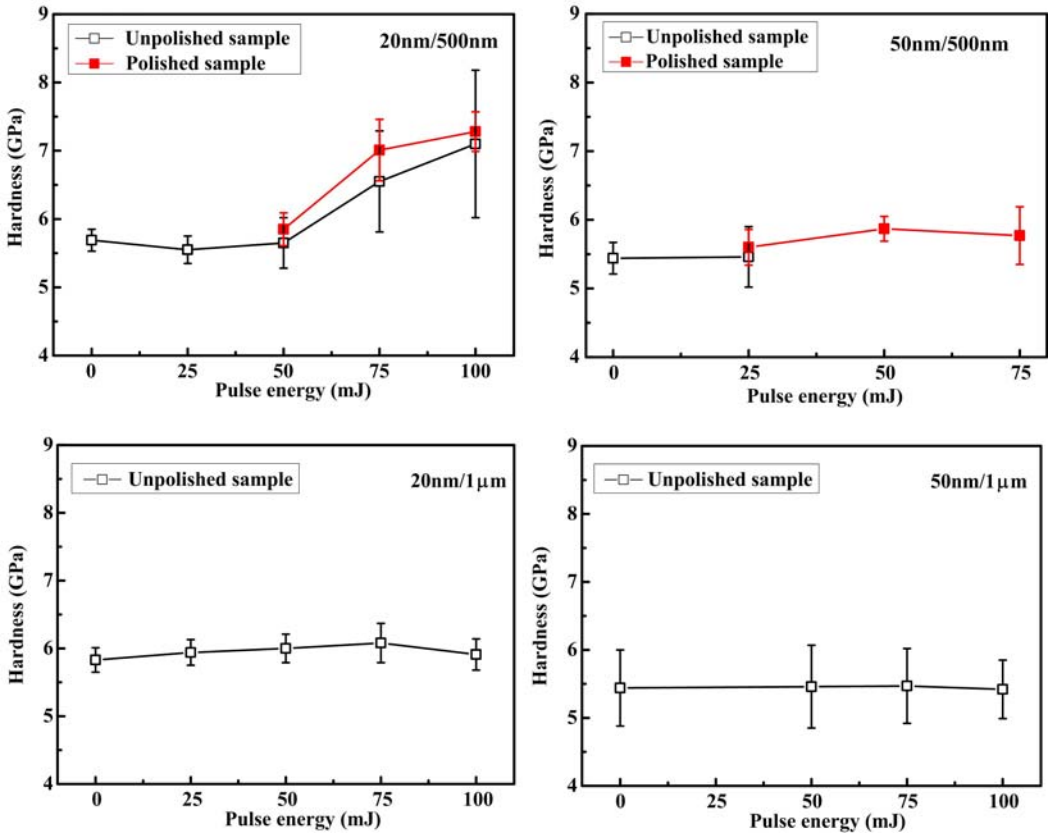

Fig. 6 Hardness as a function of laser pulse energy for both non-treated and laser-treated 500nm and 1μm thick Ti/Ni multilayer films with layer thickness of 20nm and 50nm, respectively

2.4 Discussions

Significant thickness effects were observed in the microstructural and mechanical properties for laser-treated Ti/Ni multilayer thin films. The observed effects are likely resulted from the different thermal energy distribution in the multilayers. After a single pulse, ultrahigh temperature is generated on the irradiated surface, and the resulting thermal wave propagates toward the substrate, while a significant amount of thermal energy is still confined near the surface region. With successive pulses, energy continues to accumulate in this area, promoting the formation of an intermixed layer. Meanwhile, for multilayers, interface reactions play an important role in thermal energy dissipation

via interdiffusion, intermixing and intermetallic formation[38, 39]. Films with thin layers and a larger number of interfaces dissipate more energy, resulting in less energy accumulation in the intermixed region. For thick films, the longer heat conduction distance and increased number of interfaces left even less energy near the surface. Consequently, tailoring the thickness of metallic multilayer thin films can be a powerful means in the functionalization of laser-treated material systems in desired applications.

Applying these postulations, we attempt to discuss the intermixed layer formation and the surface strengthening of laser-treated multilayers. For the 1μm thick films, thermal energy is conducted deep into the multilayer stack, leaving insufficient energy near the surface, thus the formation of a smooth, thin intermixed layer. For the 500nm thick films, the intermixed layer is thicker due to more energy confined near the surface. Intermetallic precipitation is the main factor for improving surface strength, but it does require a critical energy to initiate. There are a larger number of interfaces in films with λ =20nm, and more energy is consequently absorbed along the interfaces, leading to less accumulated energy in the intermixed layer. As a result, higher pulse-energy is required to initiate the intermetallic formation. This explains why the intermetallic phase appears after laser treatment with 75mJ in the 20nm/500nm multilayers, while at 50mJ in the 50nm/500nm case. For the 1μm thick films, the pulse energy applied in this study appears to be too low to initiate intermetallic formation and subsequent strengthening.

For the surface morphology in laser-treated multilayers, available literature attributed the periodic surface structure to the interference between the incident beam and the scattered beam on the sample surface[40]. The competition between this optical interference and the net thermal energy seems to dictate the formation of the LIPSS or the melted surface. For the 1μm thick films, as thermal conduction carries much of the energy deep into the film, less energy remains on the surface, promoting LIPSS formation for a wide range of pulse-energies. In contrast, for the 500nm films, high energy and temperature resulted on the surface leads to a rougher and more melted morphology. Low thermal energy on the surface could be the key to form LIPSS, and it is well accepted that the period Δ and orientation of the ripples depend on the wavelength Λ, the incident angle θ and the polarization of the laser beam[41]. For example, after p-polarized laser beam treatment, ripple structure with orientation parallel to polarization (vertical in the current case) can be observed with a period calculated by $\Delta=\frac{\Lambda}{\cos\theta}$. However, none of the ripples observed in this work agree with the prediction from the classic theory, indicating the properties of the multilayer films play a role in the LIPSS formation in addition to the properties of the incident laser beam. A similar phenomenon was also observed in other works related to laser-treated multilayer films[34], and further research into LIPSS on multilayers is required.

The surface oxidation observed in the 50nm/500nm films is likely from (1) surface segregation of Ti and formation of TiO_2 due to its affinity to oxygen, and (2) laser-induced ablation of the Ni layer and thermal driven Ni atomic diffusions. The TiO_2 phase was detected only in the 50nm/500nm case after treatment with 75mJ. In the 20nm/500nm case, most of the Ti material likely reacts with Ni to form the Ti-Ni alloy before exposure on the surface. In the 1μm thick films, the accumulated thermal energy on the film surface is relatively low and as a result, less Ni material is ablated and diffused, resulting in less Ti exposure.

3 Conclusion

Both film thickness and layer thickness play important roles in the microstructural and mechanical

properties of laser-treated Ti/Ni multilayer thin films. The following summarizes the main findings of this work:

(1) For thick films (h=1μm), distinct cross-hatched patterns were observed on the surface and a thin, smooth intermixed layer uniformly overlaid the multilayers under a wide range of pulse-energy treatments.

(2) For thin films (h=500nm), an indistinct ripple structure on the surface and uniform intermixing on the cross-section were observed under low pulse-energy treatment, while a massively melted surface and rough, non-uniform intermixed cross-section were observed under high pulse-energy treatment.

(3) Surface morphology results from the competition between optical interference and thermal melting. Periodic surface structures can be observed in thick films as well as in thin films with low pulse-energy due to less thermal energy accumulated on the surface, while melted surfaces were observed on the surface in thin films with high pulse-energy, especially for films with thick layers (λ=50nm).

(4) Surface strengthening occurs due to the precipitation of Ti-Ni intermetallics. Without intermetallic formation in thick films, no obvious hardness change is observed even with the intermixed layer. An obvious strengthening is achieved in thin films, especially in films with smaller layer thickness (λ=20nm) due to more intermetallic precipitation at the interfaces.

(5) Formation of the intermetallics requires a critical energy. In thick films, long heat conduction distance and a large number of interfaces lead to insufficient energy near the surface to initiate intermetallic formation. In thin films, for a given layer thickness, a critical pulse-energy is required to introduce the intermetallic phase and subsequent strengthening.

Acknowledgement

The authors would like to acknowledge the financial support of the University of Washington regents. Part of this work was conducted at the Molecular Analysis Facility, a National Nanotechnology Coordinated Infrastructure site at the University of Washington which is supported in part by the National Science Foundation (grant ECC-1542101), the University of Washington, the Molecular Engineering & Sciences Institute, the Clean Energy Institute, and the National Institutes of Health.

Reference:

[1] Hashida M, Miyasaka Y, Ikuta Y, et al. Crystal structures on a copper thin film with a surface of periodic self-organized nanostructures induced by femtosecond laser pulses[J]. Physical Review B, 2011, 83(23):235413.

[2] Jee Y, Becker M F, Walser R M. Laser-induced damage on single-crystal metal surfaces[J]. Journal of the Optical Society of America B, 1988, 5(3):648-659.

[3] van Driel H M, Sipe J E, Young J F. Laser-induced periodic surface structure on solids: a universal phenomenon [J]. Physical Review Letters, 1982, 49(26):1955-1958.

[4] Tsibidis G D, Barberoglou M, Loukakos P A, et al. Dynamics of ripple formation on silicon surfaces by ultrashort laser pulses in subablation conditions[J]. Physical Review B, 2012, 86(11):115316.

[5] Birnbaum M. Semiconductor surface damage produced by ruby lasers[J]. Journal of Applied Physics, 1965, 36 (11):3688-3689.

[6] Emmony D C, Howson R P, Willis L J. Laser mirror damage in germanium at 10.6μm[J]. Applied Physics Letters, 1973, 23(11):598-600.

[7] Costache F, Henyk M, Reif J. Modification of dielectric surfaces with ultra-short laser pulses[J]. Applied Surface

Science, 2002, 186(1-4):352－357.

[8] Temple P, Soileau M J. Polarization charge model for laser-induced ripple patterns in dielectric materials[J]. Quantum Electronics, IEEE Journal of, 1981, 17(10):2067－2072.

[9] Chen X Y, Lu Y F, Cho B J, et al. Pattern-induced ripple structures at silicon-oxide/silicon interface by excimer laser irradiation[J]. Applied Physics Letters, 2002, 81(7):1344－1346.

[10] Brugger J, Berenschot J W, Kuiper S, et al. Resistless patterning of sub-micron structures by evaporation through nanostencils[J]. Microelectronic Engineering, 2000, 53(1-4):403－405.

[11] Benjamin R, Véronique B, Jean-Baptiste D, et al. Study of SU-8 reliability in wet thermal ambient for application to polymer micro-optics on VCSELs[J]. Japanese Journal of Applied Physics, 2014, 53(8S2):08MC03.

[12] Gittard S D, Narayan R J. Laser direct writing of micro- and nano-scale medical devices[J]. Expert review of medical devices, 2010, 7(3):343－356.

[13] Harris M L, Doraiswamy A, Narayan R J, et al. Recent progress in CAD/CAM laser direct-writing of biomaterials[J]. Materials Science and Engineering:C, 2008, 28(3):359－365.

[14] Watkins K G, McMahon M A, Steen W M. Microstructure and corrosion properties of laser surface processed aluminium alloys: a review[J]. Materials Science and Engineering:A, 1997, 231(1-2):55－61.

[15] Mondal A K, Kumar S, Blawert C, et al. Effect of laser surface treatment on corrosion and wear resistance of ACM720 Mg alloy[J]. Surface and Coatings Technology, 2008, 202(14):3187－3198.

[16] Dutta Majumdar J, Manna I. Laser surface alloying of copper with chromium II. Improvement in mechanical properties[J]. Materials Science and Engineering:A, 1999, 268(1-2):227－235.

[17] Tong X, Dai M J, Zhang Z H. Thermal fatigue resistance of H13 steel treated by selective laser surface melting and CrNi alloying[J]. Applied Surface Science, 2013, 271(8):373－380.

[18] Fu Y, Batchelor A W. Laser alloying of aluminum alloy AA 6061 with Ni and Cr. Part II. The effect of laser alloying on the fretting wear resistance[J]. Surface and Coatings Technology, 1998, 102(1-2):119－126.

[19] Trtica M, Gakovic B, Batani D, et al. Surface modifications of a titanium implant by a picosecond Nd:YAG laser operating at 1064 and 532nm[J]. Applied Surface Science, 2006, 253(5):2551－2556.

[20] Dutta Majumdar J, Manna I. Laser surface alloying of copper with chromium: I. Microstructural evolution[J]. Materials Science and Engineering:A, 1999, 268(1-2):216－226.

[21] Fu Y, Batchelor A W, Gu Y, et al. Laser alloying of aluminum alloy AA 6061 with Ni and Cr. Part 1. Optimization of processing parameters by X-ray imaging[J]. Surface and Coatings Technology, 1998, 99(3):287－294.

[22] Rao S I, Hazzledine P M. Atomistic simulations of dislocation-interface interactions in the Cu-Ni multilayer system [J]. Philosophical Magazine A: Physics of Condensed Matter, Structure, Defects and Mechanical Properties, 2000, 80(9):2011－2040.

[23] Yang Z, Lian J, Wang J. Molecular dynamics simulation of thin film interfacial strength dependency on lattice mismatch[J]. Thin Solid Films, 2013, 537:190－197.

[24] Shaomin X, Bogy D B. Experimental study of head-disk interface in heat-assisted magnetic recording[J]. IEEE Transactions on Magnetics, 2014, 50(3):148－154.

[25] Troche P, Hoffmann J, Heinemann K, et al. Thermally driven shape instabilities of Nb/Cu multilayer structures: instability of Nb/Cu multilayers[J]. Thin Solid Films, 1999, 353(1):33－39.

[26] Yang Z, Wang J. Orientation-dependent hardness in as-deposited and low-temperature annealed Ti/Ni multilayer thin films[J]. Journal of Applied Mechanics, 2015, 82(1):011008.

[27] Liu Y, Bufford D, Wang H, et al. Mechanical properties of highly textured Cu/Ni multilayers[J]. Acta Materialia, 2011, 59(5):1924－1933.

[28] Misra A, Hirth J P, Hoagland R G. Length-scale-dependent deformation mechanisms in incoherent metallic multilayered composites[J]. Acta Materialia, 2005, 53(18):4817－4824.

[29] Yang Z, Wang J. Coupled annealing temperature and layer thickness effect on strengthening mechanisms of Ti/Ni multilayer thin films[J]. Journal of the Mechanics and Physics of Solids, 2016, 88:72－82.

[30] Yang Z, Stossel M, Wang J. Microstructural evolution and surface strengthening of pulse-laser treated Ti/Ni

multilayer thin films[J]. Extreme Mechanics Letters, 2015, 4:45－51.

[31] Petrović S, Gakovi ć B, Kovacč J, et al. Synthesis of ultra-thin oxide layer in laser-treated 3× (Al/Fe)/Si multilayer structure[J]. Journal of Materials Science, 2014, 49(22):7900－7907.

[32] Petrović S, Peruško D, Kovač J, et al. Laser treatment of nanocomposite Ni/Ti multilayer thin films in air[J]. Surface and Coatings Technology, 2012, 211:93－97.

[33] Kietzig A-M, Hatzikiriakos S G, Englezos P. Patterned superhydrophobic metallic surfaces[J]. Langmuir, 2009, 25(8):4821－4827.

[34] Petrović S, Radak B, Peruško D, et al. Laser-induced surface alloying in nanosized Ni/Ti multilayer structures [J]. Applied Surface Science, 2013, 264:273－279.

[35] Čizmović M, Kovač J, Milosavljević M, et al. Intermixing in Al/Ti multilayer structures induced by nanosecond laser pulses[J]. Physica Scripta, 2013, 2013(T157):014008.

[36] Jergel M, Anopchenko A, Majková E, et al. Excimer laser treated Ag/Co multilayers exhibiting giant magnetoresistance effect[J]. Superficies y Vacío, 1999, 9:193－198.

[37] Oliver W C, Pharr G M. An improved technique for determining hardness and elastic modulus using load and displacement sensing indentation experiments[J]. Journal of Materials Research, 1992, 7(6):1564－1583.

[38] Catalina F, Afonso C N, Serna R, et al. Kinetics of laser induced interface reactions in Sb/Ge thin multilayer films [J]. Surface Science, 1991, 251-252:1006－1011.

[39] Afonso C N, Catalina F, Petford-Long A K, et al. Laser induced interface reactions in Sb/Ge multilayer thin films: a study by RBS and CS-TEM[J]. Nuclear Instruments & Methods in Physics Research, 1992, 64 (1-4): 807－810.

[40] Sipe J E, Young J F, Preston J S, et al. Laser-induced periodic surface structure. I. Theory[J]. Physical Review B, 1983, 27(2):1141－1154.

[41] Skolski J Z P, Römer G R B E, Obona J V, et al. Laser-induced periodic surface structures: Fingerprints of light localization[J]. Physical Review B, 2012, 85(7):075320.